




Combined enhancement of ascorbic acid, β -carotene and zeaxanthin in gene-edited lettuce

Yarin Livneh¹ , Ehud Leor-Librach¹, Dor Agmon¹, Tal Makov-Bouaniche², Vivekanand Tiwari³, Ekaterina Shor³, Yelena Yeselson³, Tania Masci¹, Arthur Schaffer³, Dana Charuvi³ , Joseph Hirschberg²  and Alexander Vainstein^{1,*}

¹Institute of Plant Sciences and Genetics in Agriculture, The Robert H. Smith Faculty of Agriculture, Food and Environment, The Hebrew University of Jerusalem, Rehovot, Israel

²Department of Genetics, Alexander Silberman Institute of Life Sciences, The Hebrew University of Jerusalem, Rehovot, Israel

³Institute of Plant Sciences, Agricultural Research Organization (ARO), Volcani Center, Rishon LeZion, Israel

Received 7 October 2024;

revised 12 January 2025;

accepted 5 February 2025.

*Correspondence (Tel +97289489082;

fax +97289489899; email alexander.

vainstein@mail.huji.ac.il)

Summary

Lettuce is widely grown and consumed but provides lower nutritional value compared to other leafy greens, particularly in the essential vitamins A and C. To address this, major control points in carotenoid and ascorbic acid (AsA) production were targeted using a viral-based CRISPR/Cas9 system in the commercial lettuce cultivar 'Noga'. Knockout of *lycopene ϵ -cyclase* (*LCY- ϵ*), the enzymatic gatekeeper opposing production of β -branch carotenoids, increased β -carotene (provitamin A) levels up to 2.7-fold and facilitated zeaxanthin accumulation up to 4.3 $\mu\text{g/g}$ fresh weight. Chlorophyll fluorescence measurements revealed that photosystem II efficiency was unaffected in *LCY- ϵ* mutants, though their non-photochemical quenching (NPQ) capacity decreased at light intensities above 400 $\mu\text{mol m}^{-2} \text{s}^{-1}$. However, the gene-edited plants exhibited normal growth and comparable plant mass, despite the absence of two major lettuce xanthophylls, lutein and lactucaxanthin. Modifications in a regulatory region in the upstream ORF of *GDP-L-galactose phosphorylase 1 and 2* (*uGGP1* and *uGGP2*), the rate-limiting enzyme in AsA production, resulted in an average 6.9-fold increase in AsA levels. The mutation in *uGGP2* was found to dominantly influence AsA over-accumulation. Knockout lines that combined the mutations in *LCY- ϵ* , *uGGP1*, *uGGP2* and in *carotenoid cleavage dioxygenase 4a* (*CCD4a*), an isozyme involved in β -carotene degradation in lettuce, exhibited significantly enhanced content of AsA, β -carotene and zeaxanthin. Our results demonstrate the potential of multi-pathway gene editing to 'supercharge' economically important crops such as lettuce as a means to address micronutrient deficiencies in modern diets.

Keywords: ascorbic acid, biofortification, CRISPR, lettuce, zeaxanthin, β -carotene.

Introduction

In the relentless pursuit of crop improvement, emerging gene editing technologies are swift and precise methods for molecular breeding, especially with clustered regularly interspaced palindromic repeats (CRISPR)/CRISPR associated (Cas) systems (henceforth CRISPR; Lyzenga *et al.*, 2021). By using CRISPR, numerous instances of crop enhancements have been documented, resulting in augmented traits such as greater yield, disease resistance, abiotic stress tolerance, agriculture-friendly plant architecture and more (Mishra and Pandey, 2024). Gene editing is also a valuable tool in addressing the contemporary concern of 'hidden hunger' or micronutrient deficiency, affecting at least 20% of the global population (Jiang *et al.*, 2021; Scharff *et al.*, 2022). Two major nutrients lacking in modern diets are vitamin A, which can be metabolized from the orange carotenoid β -carotene (Grune *et al.*, 2010) and vitamin C, i.e. ascorbic acid (AsA; Rowe and Carr, 2020b).

Carotenoids are plant-derived pigments with crucial roles in human health. β -carotene is the main vegetal precursor of retinol (vitamin A), which is vital for night vision, cell proliferation, reproduction and embryonic development, brain and immune system function and more (Grune *et al.*, 2010; Sajovic

et al., 2022). Vitamin A deficiency may lead to blindness, morbidity and mortality, particularly in children (Carazo *et al.*, 2021). β -carotene and other carotenoids such as zeaxanthin also serve as general antioxidants against harmful reactive oxygen species (ROS; Sajovic *et al.*, 2022). Zeaxanthin is particularly concentrated in the macula of the eye's retina and shields it against blue light and oxidative stress, reducing the risk of age-related macular degeneration (AMD). Additionally, zeaxanthin has been shown to possess specific anti-cancer properties and may help slow the progression of atherosclerosis (Sajilata *et al.*, 2008).

Carotenoids synthesized in photosynthetic tissues are stored in pigment-protein complexes within the chloroplast thylakoid membranes, where they aid in light harvesting and protect against photodamage and oxidative stress. Biosynthesis starts with the condensation of two geranyl-geranyl pyrophosphate molecules into phytoene, catalysed by phytoene synthase (PSY; Rosas-Saavedra and Stange, 2016). A series of enzymatic reactions then convert phytoene into the linear carotenoid lycopene. In most plant species, biosynthesis diverges into two branches: the β -branch, producing carotenoids with two β rings catalysed by lycopene β -cyclase (*LCY- β*) and the α -branch, producing carotenoids with one β and one ϵ ring, such as lutein,

catalysed by both LCY- β and lycopene ϵ -cyclase (LCY- ϵ). The β -branch leads to the formation of β -carotene, zeaxanthin, antheraxanthin, violaxanthin, neoxanthin and the plant hormone abscisic acid (ABA; Simkin, 2021). β -carotene may also be cleaved by carotenoid cleavage dioxygenase 4 (CCD4), producing smaller, volatile apocarotenoid compounds that contribute to the aroma of some fruits and flowers (Varghese *et al.*, 2021). The xanthophylls lutein, violaxanthin and neoxanthin are incorporated into the light-harvesting complex of photosystem II (LHC II) and play a role in non-photochemical quenching (NPQ) under strong light conditions (Lokstein *et al.*, 2021). In lettuce (*Lactuca sativa*) and a few other species, a unique LCY- ϵ forms the rare xanthophyll lactucaxanthin, which contains two ϵ rings (Cunningham and Gantt, 2001; Siefermann-Harms *et al.*, 1981). It was found that lactucaxanthin accounts for about a quarter of the total xanthophylls in photosystem II of lettuce, likely replacing some lutein molecules in LHC II (Phillip and Young, 1995), with no known additional physiological functions.

Due to the importance of β -carotene in the human diet, extensive research has focused on increasing its content in crops, as demonstrated by the introduction of transgenes to create 'Golden Rice' (Amna *et al.*, 2020; Ye *et al.*, 2000). Alternatively, inhibiting LCY- ϵ or CCD4 activity through gene editing can shift carbon flux towards the β -branch in a more subtle approach. The downregulation of LCY- ϵ by RNAi or its complete knockout by CRISPR has significantly increased β -carotene in tubers, seeds and fruits of several plant species (Diretto *et al.*, 2006; Kaur *et al.*, 2020; Ke *et al.*, 2019; Yu *et al.*, 2008). Similarly, RNAi silencing or CRISPR-mediated knockout of CCD4 has turned white-fleshed fruits and flowers yellow or orange due to carotenoid accumulation (Bai *et al.*, 2016; Ohmiya *et al.*, 2006; Watanabe *et al.*, 2018).

Vitamin C, or AsA, historically recognized as the remedy for scurvy, is essential for human health. AsA acts as a potent antioxidant against ROS (Paciolla *et al.*, 2019) and functions as a cofactor in collagen formation (Drouin *et al.*, 2011), iron absorption (Lynch and Cook, 1980) and epigenetic marking (Camarena and Wang, 2016). Modern diets and food processing methods often fail to meet AsA needs, leading to vitamin C deficiency in various populations worldwide (Rowe and Carr, 2020b). Therefore, various approaches have been taken to increase its content in crops (Paciolla *et al.*, 2019).

Plants synthesize AsA as an antioxidant to counteract ROS generated during photosynthesis and oxidative metabolism, and it also regulates development and stress responses (Ntagkas *et al.*, 2018). Primarily biosynthesized via the D-mannose/L-galactose pathway, AsA production begins with D-glucose undergoing a series of enzymatic reactions. The first dedicated step and a key regulatory control point in this process is the phosphorylation of GDP-L-galactose by GDP-L-galactose phosphorylase (GGP), forming L-galactose-1-P. Subsequent enzymatic steps complete the transformation into L-Ascorbate, the ionized form of AsA (Mellidou and Kanellis, 2017).

Laing *et al.* (2015) identified an upstream open reading frame (uORF) with a non-canonical start codon in the 5' untranslated region (5'UTR) of the gene coding for GGP in *Arabidopsis thaliana*. This uORF encodes a highly conserved peptide involved in a negative feedback loop that regulates AsA levels. The authors proposed a post-transcriptional mechanism in which high levels of AsA affect the translation of the uORF, which in turn inhibits GGP synthesis. Different modifications to the uORF were generated by

CRISPR, resulting in increased foliar AsA levels in *A. thaliana*, *Solanum pimpinellifolium* and lettuce (Li *et al.*, 2018; Zhang *et al.*, 2018).

Lettuce is a significant agricultural crop of the Asteraceae family, grown and consumed worldwide. Vitamin content in lettuce varies based on cultivar, growth conditions, harvest time and storage, but other leafy greens such as kale, spinach and chard are nutritionally superior in general (Carazo *et al.*, 2021; Ferland and Sadowski, 1992; Khanam *et al.*, 2012; Kim *et al.*, 2016b; Rowe and Carr, 2020a). Only a few vegetables contain meaningful amounts of zeaxanthin (Morand-Laffargue *et al.*, 2023), and it is usually not detected or found in very small amounts in lettuce (Kim *et al.*, 2016a). Although many studies focus on the biofortification of specific vitamins, works on stacking mutations in different biosynthetic pathways to enhance multiple nutritional qualities in crops are scarce and limited to transgene overexpression approaches (Kumar *et al.*, 2022; Medina-Lozano and Díaz, 2022; Naqvi *et al.*, 2009).

In this study, we aimed to enhance the nutritional content of lettuce by targeting LCY- ϵ , uGGP and CCD4 using a viral-based CRISPR gene-editing system. We evaluated the effects of editing key regulatory points in the carotenoid and AsA pathways separately. The resultant mutant plants were crossed to stack these modifications, resulting in lettuce lines exhibiting significantly enhanced levels of AsA, β -carotene and zeaxanthin. Our approach demonstrates the efficacy of multi-pathway gene editing for biofortifying crops to combat micronutrient deficiencies.

Results

Increased β -carotene levels in knockout LCY- ϵ gene-edited lettuce

We first generated a stable Cas9-expressing lettuce cv. 'Noga' line and subsequently used it for targeting various genes using a viral vector pTRV2 carrying different single-guide RNAs (gRNAs). To determine whether knocking out LCY- ϵ would increase β -carotene content in lettuce, we employed pTRV2 carrying a gRNA designed to target the first exon of LCY- ϵ (pTRV2-LCY- ϵ). 80 explants were inoculated with pTRV2. Following regeneration, 15 plantlets were confirmed as gene-edited by sequencing, and three independent lines (L1, L2, L3) were selected for further evaluation (Figure 1a,b). These lines, which all had distinct frameshift-inducing indels leading to a premature stop codon, were self-pollinated over successive rounds to ensure homozygosity for the knockout mutation. The gene-edited lines, along with non-edited Cas9-expressing control plants (NE), were analysed for their carotenoid composition via HPLC (Figure 1c). Neither lutein nor lactucaxanthin was detected in the mutant lines. On the other hand, β -carotene increased by 2.4- to 2.7-fold in the mutant lines compared to NE plants. Violaxanthin levels approximately doubled in all of the mutants. Zeaxanthin and antheraxanthin, which were absent in control plants, accumulated in the mutant lines, reaching up to 4.3 and 9.4 $\mu\text{g/g}$ fresh weight (FW), respectively. Neoxanthin levels did not differ significantly between NE and mutant lines. We performed a GC-MS analysis of a β -ionone levels on the knockout line with a 1-bp insertion, L3. The level of this volatile cleavage product of β -carotene almost doubled (97.2% increase) as compared to control plants (Figure S1). To assess the impact of the LCY- ϵ knockout at the transcriptional level, we analysed the expression

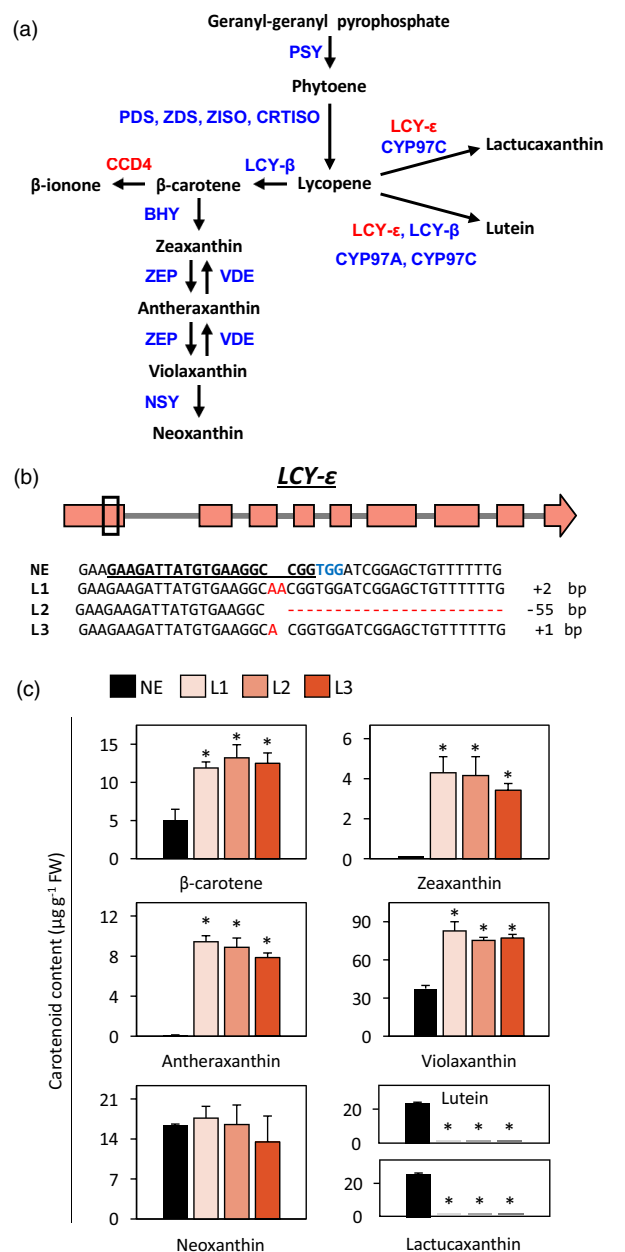


Figure 1 Enhancement of β -branch carotenoids in *LCY-ε* gene-edited lettuce plants. (a) A simplified scheme of the carotenoid biosynthesis pathway in lettuce and the key enzymes involved in the process. PSY, phytoene synthase; PDS, phytoene desaturase; ZDS, ζ -carotene desaturase; ZISO, ζ -carotene isomerase; CRTISO, carotenoid isomerase; LCY- β , lycopene β -cyclase; BHY, β -carotene hydroxylase; ZEP, zeaxanthin epoxidase; VDE, violaxanthin de-epoxidase; NSY, neoxanthin synthase; CCD4, carotenoid cleavage deoxygenase 4; LCY- ϵ , lycopene ϵ -cyclase; CYP97A and CYP97C, cytochrome P450 enzymes. (b) Top: schematic representation of the *LCY-ε* gene structure. Bottom: sequences of *LCY-ε* in non-edited (NE) and CRISPR-generated mutant lettuce lines L1, L2 and L3. The gRNA spacer sequence, located in the first exon of the gene (black rectangle), is underlined. Blue font, PAM sequence; red font, indels. The length of indels for each line is indicated to the right. (c) HPLC analysis of carotenoid content in leaves of 2-month-old NE and *LCY-ε* gene-edited lettuce lines. Bars represent means of *n* = 3 biological replicates \pm SD. Asterisks indicate statistically significant differences between independent homozygous gene-edited lines and control counterparts (Dunnett's test, *p* ≤ 0.05). NE, non-edited.

patterns of key biosynthetic enzymes in the carotenoid pathway in gene-edited and NE lines using RT-qPCR (Figure S2). The relative expression of the *LCY-ε* transcript decreased dramatically in the three mutant lines. No significant changes were observed across the mutant lines in the expression of other analysed genes, *PSY*, *LCY-β*, *CCD4*, β -carotene hydroxylase (*BHY*), zeaxanthin epoxidase (*ZEP*) and violaxanthin de-epoxidase (*VDE*).

The gene-edited lettuce plants grew normally and appeared visibly similar to the NE plants (Figure 2a). To examine the effect of the suppression of accumulation of lutein and lactucaxanthin on photosynthetic activity, total chlorophyll content and the chlorophyll *a/b* ratio were analysed and found consistent across gene-edited and control lines (Table 1). The maximum quantum yield of PSII (F_v/F_m) was also similar between all lines, indicating comparable PSII efficiency (Table 1). We also calculated NPQ from chlorophyll fluorescence measurements, including response to varying light intensities, induction and relaxation kinetics, in mutant and control NE plants (Figure 2b–e). The NPQ response of the mutant lines in increasing light intensities of up to 400 $\mu\text{mol/m}^2/\text{s}$ was not different from control lines. At higher light intensities, NPQ in the mutant lines was significantly lower compared to the control (Figure 2b). When comparing NPQ induction kinetics at an actinic light of 530 $\mu\text{mol/m}^2/\text{s}$, the mutant plants exhibited a rapid induction that plateaued within 180 s; however, they reached a considerably lower maximum NPQ capacity than the control (Figure 2c). The quantum yield efficiency of PS II [$Y(II)$] and electron transfer rate (ETR) were higher in mutant lines compared to the control (Figure 2d,e). During the growth period, daily maximum light intensity in the greenhouse ranged from 174 to 457 $\mu\text{mol/m}^2/\text{s}$, with an average of 300 $\mu\text{mol/m}^2/\text{s}$. Under these conditions, the total plant mass at harvest of the *LCY-ε* mutant lines was similar to that of the NE control plants (Table 1), with comparable leaf number and leaf length (Table S1).

Generation of AsA-enhanced lettuce plants in *LCY-ε* knockout background

Lettuce has two copies of the gene encoding GGP, *GGP1* and *GGP2* (Zhang et al., 2018; Figure 3a,b). The uORFs found in *GGP1* (uGGP1) and *GGP2* (uGGP2) share 86.2% peptide sequence homology and 84.6% identity at the nucleotide level (Figures S3 and S4). A single gRNA targeting the highly conserved region in both uORFs was designed and used to generate four independent genome-edited lines: lines A1 and A2, mutated in both uGGP1 and uGGP2, and lines A3 and A4, mutated only in uGGP2 (Figure 3a). All mutations disrupted the conserved peptide's reading frame.

Leaves from mature plants of the genome-edited lines were compared with control NE plants for their AsA content by HPLC analyses (Figure 3c). The AsA content in all mutated lines was significantly higher than in the control, with increases ranging from 5.7- to 8.4-fold. The AsA content in the double-mutant uORF lines (A1, A2) was not statistically different from that in the lines mutated only in uGGP2 (A3, A4), suggesting no cumulative effect from the additional mutation in uGGP1. To examine the effect of the mutations at the transcriptional level, we compared the relative expression of *GGP1* and *GGP2* in the double-mutant line A2, the single-mutant line A4 and NE plants by RT-qPCR (Figure 3d). The relative expression of *GGP2* nearly tripled in uGGP2 mutant line A4 compared to NE, while *GGP1* was not affected. In the double uGGP1/uGGP2 mutant line A2, the transcript levels of both *GGP1* and *GGP2* had tripled. Since the

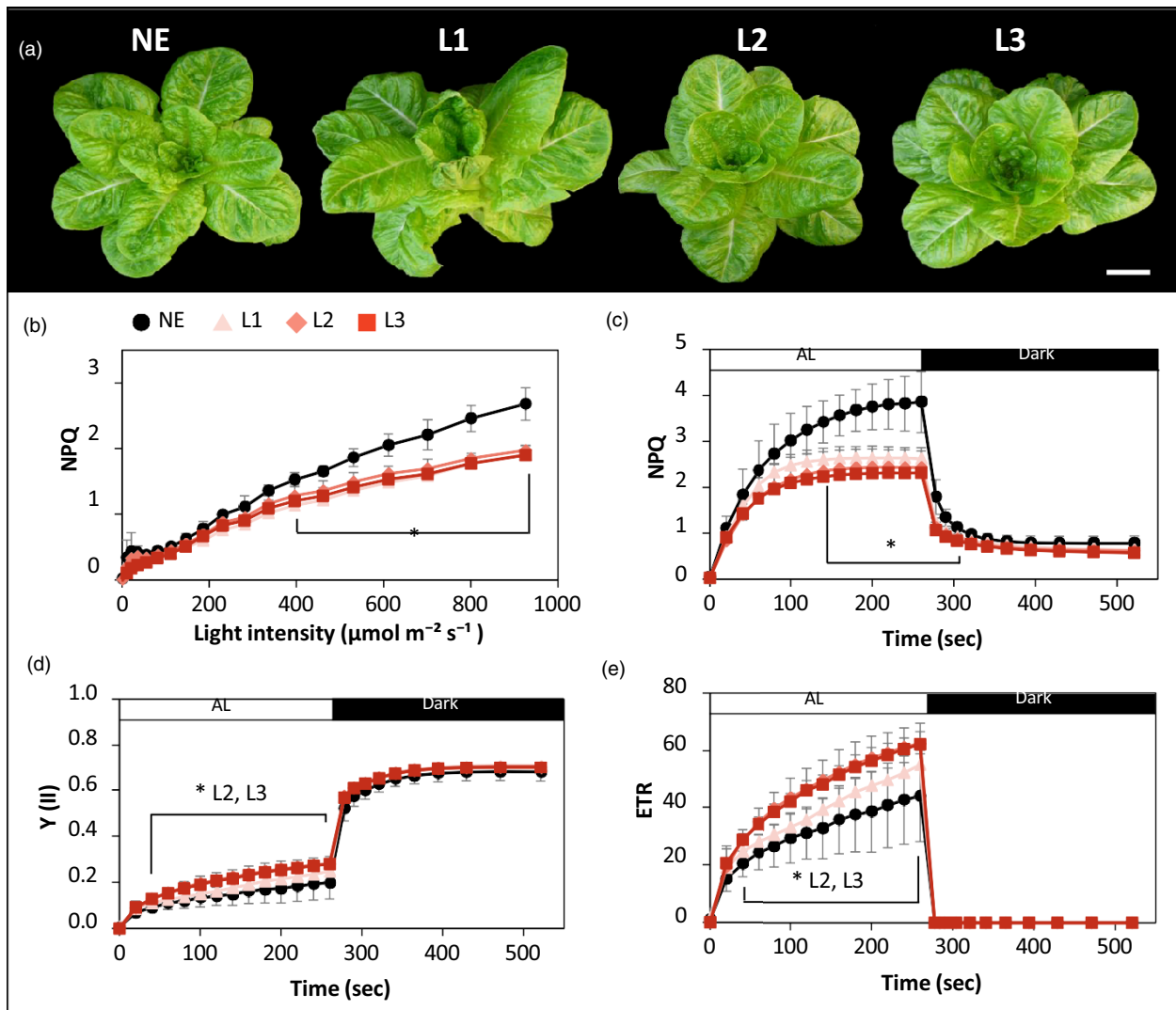


Figure 2 Photosynthetic characteristics of *LCY-ε* gene-edited lettuce plants. (a) Images of two-month-old non-edited (NE) and *LCY-ε* mutant lines L1, L2 and L3. Bar = 10 cm. (b) Light curve of non-photochemical quenching (NPQ) in dark-adapted leaves. (c) Induction and relaxation of NPQ in dark-adapted leaves. (d) Induction curve of quantum yield of PSII [Y(II)]. (e) Induction curve of electron transport rate (ETR). (b–e) Data are means \pm SD ($n = 4$). Asterisk (*) marks significant differences from NE plants (Dunnett's test, $P \leq 0.05$). White and black bars at the top of induction curves indicate actinic light (AL; $530 \mu\text{mol photons/m}^2/\text{s}$) and dark periods, respectively.

Table 1 Chlorophyll content, maximum quantum efficiency of photosystem II (PSII) and whole plant mass of *LCY-ε* two-month-old mutant lines. Chl, chlorophyll; FW, fresh weight. Data are means \pm SD ($n = 3$ –5)

Line	Chl a ($\mu\text{M/g FW}$)	Chl b ($\mu\text{M/g FW}$)	Total Chls ($\mu\text{M/g FW}$)	Chl a/b ratio	F_v/F_m	Plant mass (g)
NE	1.15 ± 0.06	0.51 ± 0.04	1.66 ± 0.10	2.2 ± 0.11	0.76 ± 0.03	180.6 ± 27.7
L1	1.21 ± 0.12	0.53 ± 0.05	1.74 ± 0.17	2.2 ± 0.06	0.78 ± 0.01	179.4 ± 29.5
L2	1.13 ± 0.07	0.51 ± 0.06	1.65 ± 0.12	2.2 ± 0.19	0.79 ± 0.01	165.4 ± 27.5
L3	1.21 ± 0.05	0.55 ± 0.02	1.76 ± 0.07	2.2 ± 0.07	0.78 ± 0.01	187.2 ± 38.1

combined uORF disruptions did not further enhance AsA levels compared with just uGGP2 mutated lines, a certain upper limit for AsA levels in lettuce leaves under native metabolic flux conditions may be suggested.

To generate lettuce plants with increased AsA content in the background of β -carotene-enhanced plants, we stacked the mutations in *LCY-ε* and uGGP2 by crossing the lines with the highest increase in β -carotene (L2; 2.7-fold increase) and AsA

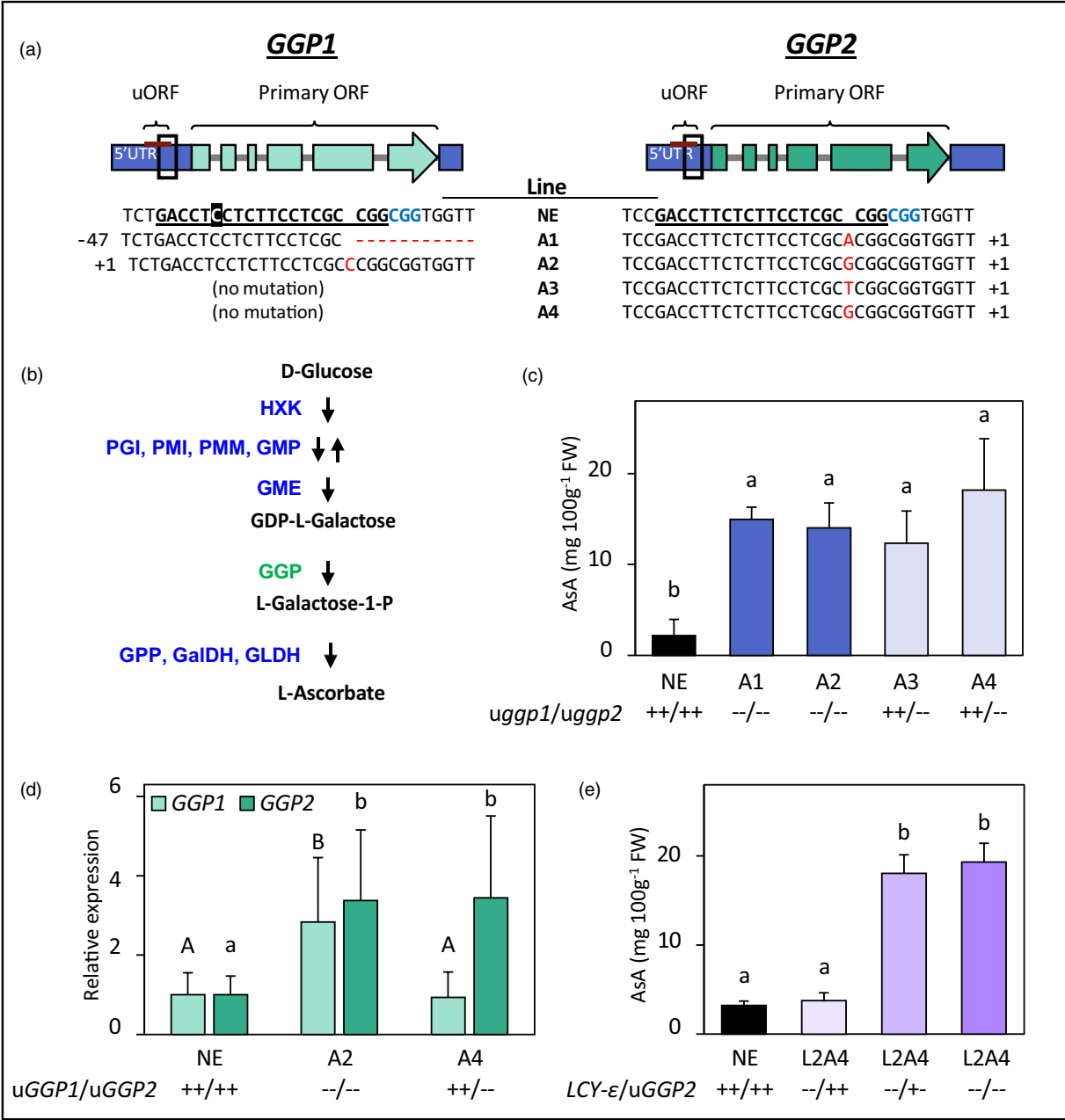


Figure 3 Ascorbic acid (AsA) content and gene expression analysis in *uGGP1* and *uGGP2* gene-edited plants. (a) Schematic representation of *GGP1* and *GGP2* gene structures and sequences in non-edited (NE) and CRISPR-generated mutant lines A1, A2, A3 and A4. The upstream open reading frame (uORF) location in the 5' untranslated region (5'UTR) is indicated with a burgundy line. The gRNA spacer sequence location in the uORF (black rectangle) is underlined, with one mismatch site in *uGGP1* noted by a black background. Blue font, PAM sequence; red font, indels. The length of indels for each line is indicated to the left (*uGGP1*) or right (*uGGP2*) of each gene. (b) Schematic illustration of the conversion of D-glucose into AsA through the D-mannose/L-galactose biosynthetic pathway. HXK, hexokinase; PGI, phosphoglucose isomerase; PMI, mannose-6-phosphate isomerase; PMM, phosphomannomutase; GMP, GDP-D-mannose pyrophosphorylase; GME, GDP-D-mannose-3' 5'-epimerase; GGP, GDP-L-galactose phosphorylase; GPP, L-galactose-1-P phosphatase; GalDH, L-galactose dehydrogenase; GLDH, L-galactono-1,4-lactone dehydrogenase. (c) AsA content in two-month-old leaves of lines A1, A2 (homozygous mutation in both *uGGP1* and *uGGP2*; *uGGP1/uGGP2* --/--), A3 and A4 (homozygous mutation in *uGGP2* alone; *uGGP1/uGGP2* +/---), compared with non-edited (NE) control plants. Data are means \pm SD ($n = 3$). Letters mark statistically significant differences (Tukey's HSD test, $P \leq 0.05$). FW, fresh weight. (d) Relative expression of *GGP1* and *GGP2* in the double mutant line A2 (*uGGP1/uGGP2* --/--) and single mutant line A4 (*uGGP1/uGGP2* +/---) compared with NE plants. Data are means \pm SD ($n = 4$). Letters indicate significant differences (Tukey's HSD test, $P \leq 0.05$); capital and lowercase letters denote separate comparisons. (e) AsA content in two-month-old leaves of different genotypes of the L2A4 plants compared with NE plants. All three L2A4 genotypes have two mutated alleles of *LCY- ϵ* , with either no mutation in *uGGP2* (*LCY- ϵ /uGGP2* --/+ +) or one mutated allele (*LCY- ϵ /uGGP2* --/+ -) or two mutated *uGGP2* alleles (*LCY- ϵ /uGGP2* --/- -). Data are means \pm SD ($n = 4$). Letters mark statistically significant differences (Tukey's HSD test, $P \leq 0.001$).

(A4; 8.4-fold increase). The offspring were selfed to produce plants homozygous for the *LCY-ε* knockout, with varying *uGGP2* alleles: wild-type, heterozygous or homozygous. The resulting genotypes were *LCY-ε*—/*uGGP2*++ (*L2A4* —/+), *LCY-ε*—/*uGGP2*+ (*L2A4* —/+—) and *LCY-ε*—/*uGGP2*— (*L2A4* —/—). Analysis of AsA levels revealed that the *L2A4* —/+ genotype, with a mutated *LCY-ε* but unaltered *uGGP2*, had AsA content comparable to control NE plants (Figure 3e). In contrast, the *L2A4* —/+— and *L2A4* —/— genotypes showed a respective 5.6- and 6-fold increase in AsA content, not significantly different from one another, irrespective of the homozygous or heterozygous state of the *uGGP2* alleles.

Multi-gene-edited lettuce plants with enhanced β-carotene, zeaxanthin and AsA content

The lettuce genome was examined to characterize CCD4s involved in β-carotene cleavage. Considering the ambiguity in the literature regarding *CCD4* genes in lettuce (Ahrazem *et al.*, 2010; Falchi *et al.*, 2013; Huang *et al.*, 2009; Huo *et al.*, 2013; Meng *et al.*, 2023; Sawada *et al.*, 2008), and given that CCD4 is part of a large enzyme family with multiple copies in some species (Varghese *et al.*, 2021), we integrated bioinformatics and molecular analyses. *Chrysanthemum morifolium*, like lettuce, belongs to the Asteraceae family; CmCCD4a was previously shown to cleave β-carotene into β-ionone (Huang *et al.*, 2009) and RNAi silencing of *CmCCD4a* in *C. morifolium* led to a pronounced carotenoid accumulation in flowers (Ohmiya *et al.*, 2006). We therefore performed a reciprocal BLAST search using the CmCCD4a protein sequence (BAF36654.1) against the lettuce RefSeq genome, which identified four sequences with high similarity (*E*-value = 0.0). These sequences are referenced in this manuscript as CCD4a (NCBI accession number BAE72094.1), CCD4b (XP_023751666.1), CCD4c (XP_023733296.1) and CCD4d (XP_023732687.1). A phylogenetic analysis revealed that CCD4b, CCD4c and CCD4d formed a distinct subgroup, while CCD4a was more closely related to *C. morifolium* CCD4 isoforms (Figure 4). A search for the *CCD4* transcripts in a published RNA-Seq dataset procured from 1-month-old lettuce leaves revealed that *CCD4a* was highly expressed, approximately 40, 1000 or 90 times more than *CCD4b*, *CCD4c* or *CCD4d*, respectively (Park *et al.*, 2020; Figure 4b). RT-qPCR analysis of transcript levels of the four candidate genes in two-month-old wild-type lettuce cv. 'Noga' plants used in this study confirmed that *CCD4a* is the major isoform expressed in the leaves; *CCD4b*, *CCD4c* and *CCD4d* expression was barely or not at all detected (Figure 5a).

To confirm the involvement of *CCD4a* in β-ionone production based on the phylogenetic association and its expression in leaves, we designed a gRNA that targets its first exon (Figure 5b). Three mutant lines, C1, C2 and C3, each with different deletions leading to nonsense mutations, were independently generated and self-pollinated to assure homozygosity. The gene-edited plants grew normally and had comparable whole plant mass, leaf number and leaf lengths to that of non-edited control plants (Table S2). GC-MS analysis of the mutant lettuce leaves showed that all lines exhibited significantly lower β-ionone levels compared to NE control plants, revealing the involvement of this isoform in β-branch carbon flux (Figure 5c).

The mutations in *LCY-ε*, *CCD4a*, *uGGP1* and *uGGP2* were stacked together through cross-pollination (LCA population, Figure 6). Multi-gene-edited plants with knockout mutations in *LCY-ε*, *CCD4a* and one mutant allele of *uGGP2* (LCA1) had significantly higher β-carotene and AsA content compared to NE

plants (Figures 6b and S5). Zeaxanthin, undetected in the control plants, accumulated up to 8.74 μg/g FW in LCA1. Violaxanthin and antheraxanthin levels were also significantly increased. Mutations in *uGGP1*, either heterozygous (LCA2, *uGGP1*+—) or homozygous (LCA3, *uGGP1*—), on top of the *LCY-ε*, *CCD4a* and *uGGP2* mutations did not statistically further enhance carotenoid or AsA accumulation. As expected, no lutein or lactucaxanthin was detected in any of the mutated genotypes; neoxanthin levels remained stable across all edited and NE plants. The multi-gene-edited plants exhibited normal growth and were visually indistinguishable from the NE control plants (Figure 6a). No significant differences in carbon/nitrogen balance were found in the leaves of any of the LCA population genotypes and control plants, suggesting that the gene edits did not significantly affect fundamental metabolic parameters (Figure S6).

Discussion

β-Carotene (provitamin A), AsA (vitamin C) and zeaxanthin are essential nutrients often lacking in modern diets (Rowe and Carr, 2020b; Sajilata *et al.*, 2008; Zheng *et al.*, 2021). This study aimed to increase these metabolites in lettuce through multiplex gene editing, targeting several enzymes involved in carotenoid and AsA biosynthesis.

Deactivation of *LCY-ε*, whether by spontaneous mutation (Richaud *et al.*, 2018), RNAi silencing (Ke *et al.*, 2019) or CRISPR-mediated gene editing (Kaur *et al.*, 2020), has been shown to increase β-carotene and other β-branch carotenoid levels at the expense of lutein production in several plant species. Unlike most plants, lettuce uniquely produces lactucaxanthin in addition to lutein due to the specific activity of its *LCY-ε* enzyme (Siefermann-Harms *et al.*, 1981). Knocking out *LCY-ε* in this study eliminated lutein and lactucaxanthin, resulting in a 2.5-fold increase in β-carotene and the accumulation of zeaxanthin, which was absent in non-edited plants. The unchanged transcript levels of carotenoid biosynthetic enzymes, alongside increased β-ionone production, hint at a metabolic carbon flux shift towards the β-branch rather than a change in transcriptomic regulation. Similar findings in sweet potato and banana in which *LCY-ε* was down-regulated or knocked out support this conclusion (Kaur *et al.*, 2020; Ke *et al.*, 2019).

Lutein plays a critical role in stabilizing the LHCII antenna trimers and dissipating excess excitation energy through the NPQ mechanism (Dall'Osto *et al.*, 2006). Lactucaxanthin is a major carotenoid in lettuce, comprising at least 20% of total thylakoid carotenoids and is hypothesized to partially substitute for lutein in the LHCII antenna (Phillip and Young, 1995). To evaluate the impact of lutein and lactucaxanthin absence, growth and photosynthetic parameters were compared between *LCY-ε* gene-edited and NE plants. The mutants, which lacked lactucaxanthin, were visually indistinguishable from NE plants and exhibited similar whole-plant mass, chlorophyll content and *F_v/F_m* values, indicating no adverse effects on PSII efficiency under the given growth conditions. Notably, mutant lines displayed higher quantum yield efficiency of PSII [Y(II)] and electron transfer rate (ETR) than NE plants, consistent with trends observed in *A. thaliana* *LCY-ε* mutants (Pogson *et al.*, 1998). The mutants also showed a faster NPQ response to strong light, possibly driven by elevated zeaxanthin and/or antheraxanthin levels (Della-Penna, 1999; Demmig-Adams *et al.*, 2014). However, their maximal NPQ capacity was significantly reduced at light

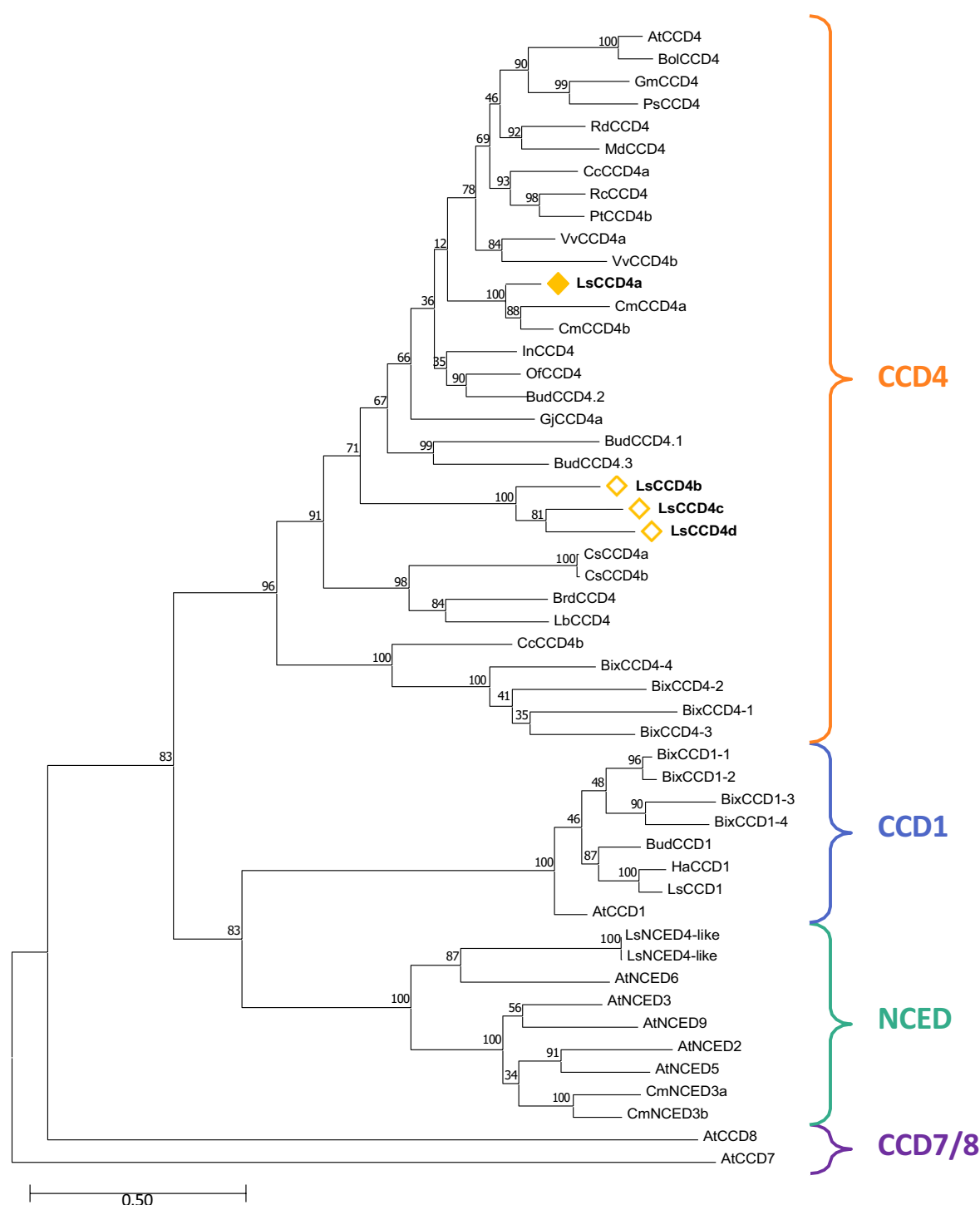


Figure 4 A neighbour-joining phylogenetic tree illustrating the relationships between lettuce CCD proteins and other plant species. Protein sequences were aligned using ClustalW, followed by phylogenetic analysis using the maximum likelihood method with 1000 bootstraps in MEGA11. Bootstrap values are indicated at branch nodes, and the scale bar represents the number of amino acid substitutions per site. At, *Arabidopsis thaliana*; Bix, *Bixa orellana*; Bol, *Brassica oleracea* var. *alboglabra*; Brd, *Brachypodium distachyon*; Bud, *Buddleja davidii*; Cc, *Citrus clementina*; Cm, *Chrysanthemum × morifolium*; Cs, *Crocus sativus*; Gj, *Gardenia jasminoides*; Gm, *Glycine max*; Ha, *Helianthus annuus*; In, *Ipomoea nil*; Lb, *Lilium brownii* var. *viridulum*; Ls, *Lactuca sativa*; Md, *Malus domestica*; Of, *Osmanthus fragrans*; Ps, *Pisum sativum*; Pt, *Populus trichocarpa*; Rc, *Ricinus communis*; Rd, *Rosa × damascena*; Vv, *Vitis vinifera*.

intensities above 400 $\mu\text{mol}/\text{m}^2/\text{s}$, aligning with reports of lower NPQ in lutein-deficient leaves of *A. thaliana* and wheat (Pogson et al., 1998; Yu et al., 2022), likely due to absence of lutein's

quenching role. Given that lettuce is the most cultivated crop in controlled environment systems (Gargaro et al., 2023), in which optimal light intensity is estimated to be between 200

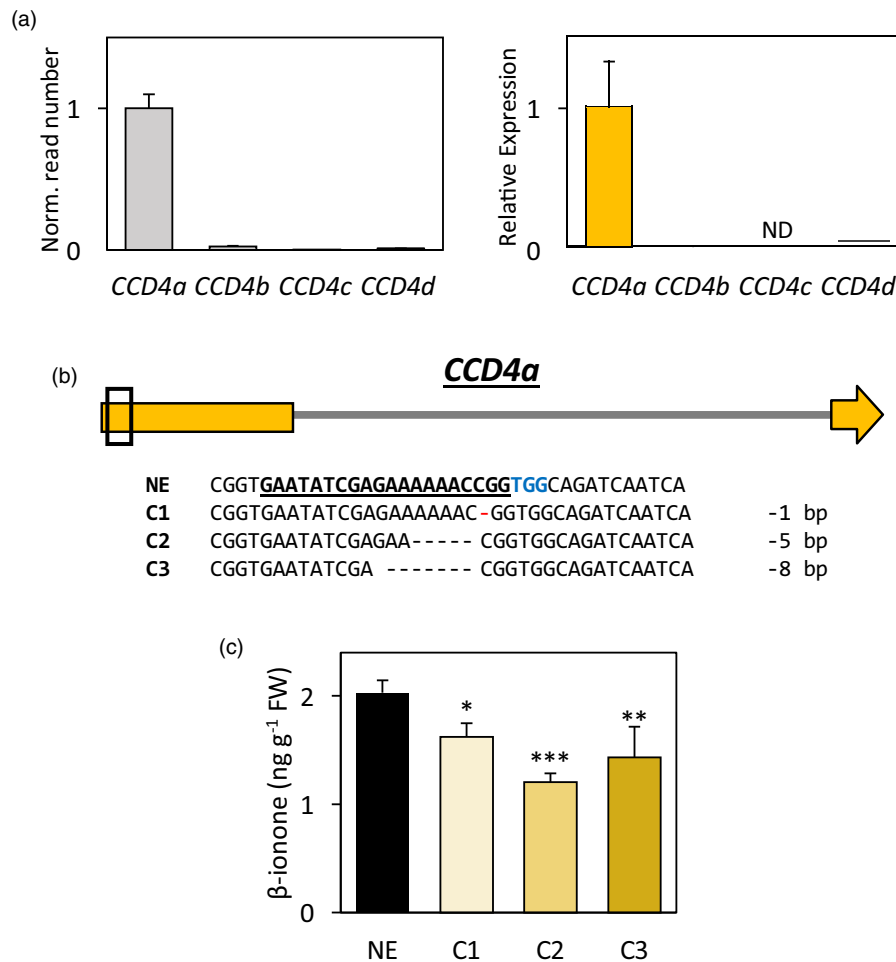


Figure 5 Analysis of three independently generated *CCD4a* gene-edited lettuce plants. (a) Relative expression of *CCD4a*, *CCD4b*, *CCD4c* and *CCD4d* in wild-type lettuce plants based on read numbers in the RNA-Seq dataset (left, Park *et al.*, 2020; cv. 'Salinas') and RT-qPCR analysis (right, current study; cv. 'Noga'). Expression was normalized to the highest expressing gene (*CCD4a*). Data are means \pm SD (RNA-Seq: $n = 3$; RT-qPCR: $n = 4$). Norm., normalized; ND, None detected. (b) Top: schematic representation of the *CCD4a* gene structure. Bottom: wild-type (non-edited, NE) and sequences of *CCD4a* mutant lines C1, C2 and C3. The gRNA spacer sequence, located in the first exon of the gene (black rectangle and arrow), is underlined. Blue font, PAM sequence; red hyphens, deletions. The number of base pair deletions for each line is indicated to the right. (c) GC-MS analysis of volatile β -ionone levels emitted from crushed lettuce leaves of lines C1, C2 and C3, compared with NE plants. Data are means \pm SD ($n = 3$). Asterisks mark significant differences (Dunnett's test, $*P \leq 0.05$, $**P \leq 0.01$, $***P \leq 0.001$).

and 250 m⁻²/s (Ahmed *et al.*, 2020), the effects of the observed alterations in NPQ are expected to be minor under these common commercial growth settings.

In the *LCY-ε* knockout lines, β -carotene content was increased by 2.4- to 2.7-fold. Previous studies on plants with deactivated *LCY-ε* consistently showed no or up to 2.7-fold increase in foliar β -carotene under non-stress conditions (Kaur *et al.*, 2020; Ke *et al.*, 2019; Yu *et al.*, 2008). In *CCD4*-mutated tobacco, the increase of β -carotene was limited to mature, senescent leaves, while carotenoid levels in younger, photosynthetic green leaves did not differ significantly from wild type (Magome *et al.*, 2023). In photosynthetic tissues, carotenoids are generally located in the thylakoid membrane of chloroplasts and plastoglobules and are coupled with chlorophylls, proteins and lipids at specific ratios, limiting the maximum β -carotene content under stable growth conditions (Lokstein *et al.*, 2021; Rottet *et al.*, 2015). Indeed, a positive correlation between chlorophyll and β -carotene levels has been observed in lettuce and other leafy crops (Brychkova

et al., 2023; Mou, 2005). In the current study, adding a *CCD4a* knockout to the *LCY-ε* mutation in the multi-gene-edited plants (LCA population) did not lead to further increases in β -carotene accumulation compared to *LCY-ε* mutant lines alone (average fold increase of 2.0 vs. 2.5, respectively), supporting this observation. This situation differs in fruits and flowers that contain chromoplasts, organelles dedicated to carotenoid storage (Rottet *et al.*, 2015). Morelli *et al.* (2024) recently demonstrated significant increases in β -carotene in lettuce leaves by converting chloroplasts to chromoplasts. Similar strategies could be combined with the mutant lines generated in this study in the future to potentially surpass the current chloroplastic limits for β -carotene and zeaxanthin content.

The activity of GGP, the first committed step in AsA production, is regulated by a conserved uORF (Laing *et al.*, 2015; Mellidou and Kanellis, 2017). Two GGP homologues, *GGP1* and *GGP2*, were previously identified and separately targeted in lettuce (Zhang *et al.*, 2018). To examine the combined effect of

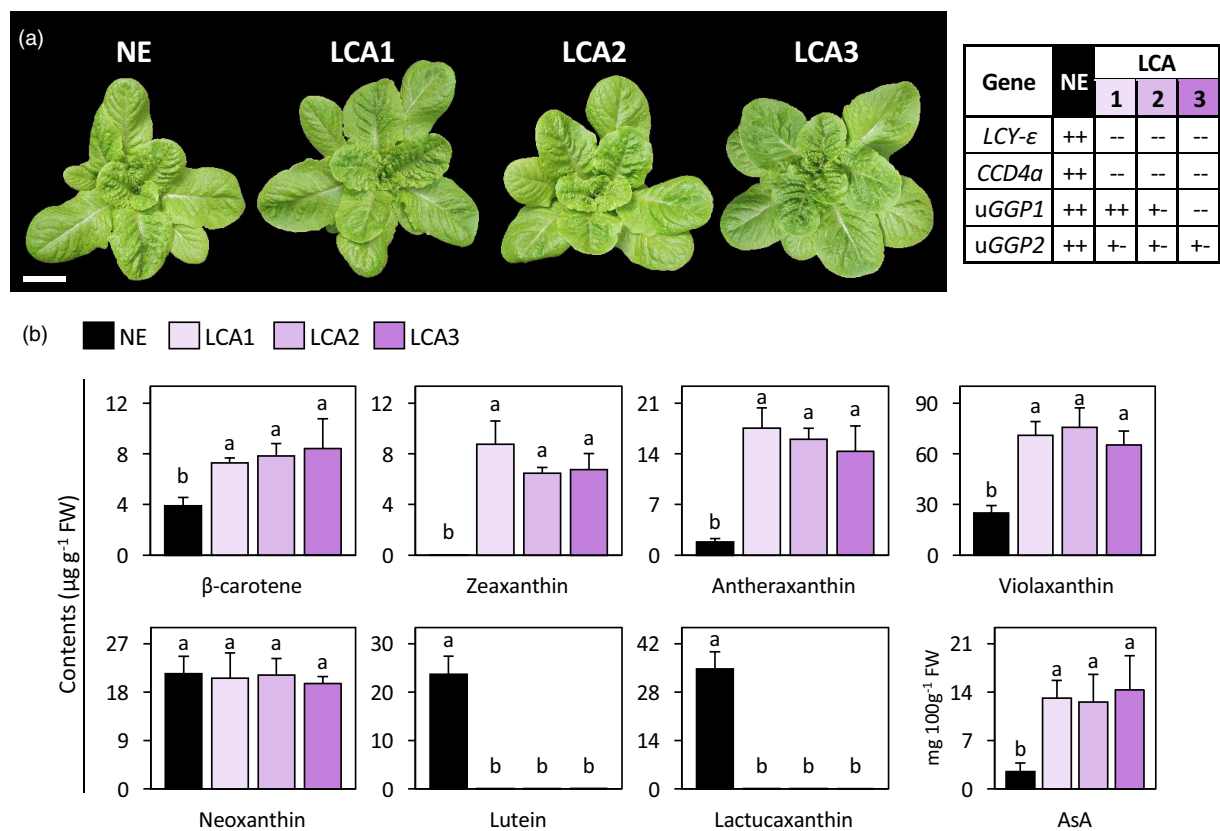


Figure 6 Carotenoid and AsA content in multi-gene-edited lettuce plants. Multi-gene-edited lettuce plants were created through cross-pollination of mutant lines with knockout mutations in *LCY-ε*, *CCD4a*, *uGGP1* and *uGGP2* (LCA population). Several genotypes were selected for carotenoid and AsA content evaluation. (a) Representative images of two-month-old control and multi-gene-edited lettuce plants LCA1, LCA2 and LCA3 (left). Bar = 10 cm. Genotype of LCA lines (right): all plants have two mutated *LCY-ε* alleles (---); two mutated *CCD4a* alleles (---); one mutated *uGGP2* allele (+-) and either no mutation in *uGGP1* (++; LCA1), one mutated allele (+-; LCA2) or two mutated alleles (---; LCA3). (b) Carotenoid and AsA content in two-month-old leaves of different genotypes of the LCA lines compared with non-edited control plants. Data are means ± SD (*n* = 3–5). Letters mark significant differences (Tukey's HSD test, *P* ≤ 0.001). NE, non-edited.

disrupting both uORFs on AsA production, we generated mutant lines with indel mutations in the conserved amino acid regions of *uGGP1* and *uGGP2*. Our results indicate that homozygous double mutants (*uGGP1/uGGP2*) have a similar effect on AsA production as a single mutated allele of *uGGP2*, with increases ranging from 5- to 8.4-fold, supporting the notion that *GGP2* is the primary isozyme responsible for AsA production in lettuce (Zhang *et al.*, 2018). Similarly, in tomato, a high-AsA phenotype was linked to a dominant mutation in the uORF of one isoform of *GGP* (Deslous *et al.*, 2021).

The exact regulatory mechanism of the conserved short uORF peptide on GGP activity, and consequently on AsA levels, remains unclear. Laing *et al.* (2015) proposed that AsA or its derivative interacts with the uORF peptide during translation, stalling the ribosome and preventing the translation of the main, enzyme-coding ORF. Alterations in the peptide's amino acid sequence may disrupt this interaction, leading to increased translation of the main ORF. Deslous *et al.* (2021) observed a higher abundance of GGP mRNA in uORF tomato mutants and suggested that mRNA stability may be enhanced in the absence of uORF regulation, allowing increased GGP translation. In the current study, the elevated transcript levels of both *GGP1* and *GGP2* in their respective uORF lettuce mutants support the latter proposal. However, Zhang *et al.* (2018) created mutants with deletions in

the non-canonical start codon region of either lettuce *uGGP1* or *uGGP2* and found that *GGP1* or *GGP2* transcript levels did not change, even in mutants with enhanced AsA content. The differing observations on mRNA steady-state levels of GGP in uORF mutants suggest that additional mechanisms might be involved in the regulation of GGP activity by the uORF.

In multi-gene-edited plants (*LCY-ε*, *uGGP2* and *CCD4a*), zeaxanthin levels were approximately doubled compared to those observed in plants with the single *LCY-ε* knockout. The increased AsA availability from the *uGGP2* mutation may have enhanced zeaxanthin accumulation, as ascorbate acts as a cofactor for VDE, the enzyme converting violaxanthin to zeaxanthin (Demmig-Adams, 1990; Smirnov and Wheeler, 2000). Alternatively, the possibility that *CCD4a* suppression creates a different distribution of carotenoids in the β-branch cannot be excluded. Zeaxanthin is less commonly available in the diet, while lutein, thought to play a role in cognition (Johnson, 2014), is typically found in most leafy vegetables (Morand-Laffargue *et al.*, 2023). Zeaxanthin is particularly concentrated in the central macula, where it is present alongside lutein in roughly equal amounts (Sajilata *et al.*, 2008). Lactucaxanthin, due to its rarity in the plant kingdom, remains largely unstudied. The lettuce genotypes developed in this study with varying ratios of lutein, zeaxanthin and lactucaxanthin offer a

unique opportunity to conduct studies within the same food matrix, potentially enabling direct comparisons of the preventative effects of the three dihydroxy xanthophylls on degenerative diseases.

A 'supercharged' lettuce enriched with zeaxanthin, β -carotene and ascorbic acid, generated through the integration of editing events in separate metabolic pathways, may represent a stepping stone towards creating crops with enhanced nutritional qualities to combat 'hidden hunger'.

Experimental procedures

Plant material and growth conditions

Romaine lettuce cv. 'Noga' seeds were kindly provided by Hazera Ltd. Seeds were sterilized and sown on germination medium (0.25× MS, 0.75% AGA03 agar [Formedium], 1% sucrose). Seedlings with two to three leaves were sampled for DNA extraction (when applicable) and transferred to cell trays with gardening soil mix for an acclimation period of 2–3 weeks. After acclimation, the plants were repotted into 12 cm cylindrical pots. The plants were grown in a greenhouse under day/night temperatures of 26/20 °C and natural lighting. Light intensity in the greenhouse was continuously monitored throughout the growth period using a HOBO Pendant Temperature Data Logger (MX2201, Onset Brands; <https://www.onsetcomp.com/>). Leaf number count and length were determined from at least four biological replicates at 6 weeks of age. Leaf number count included all leaves in the rosette that were at least 2 cm long and not completely senescent. Leaf length was measured and averaged from three middle, fully expanded leaves per plant, from the base of the leaf (at the connection point with the stem) to its tip along the midvein. Plant mass was determined from at least four biological replicates of 2-month-old plants by weighing whole lettuce heads cut just above the ground (excluding the roots). Experiments were conducted across all seasons of the year.

Plasmid construction and gRNA design

A human-optimized Cas9 (*hCas9*; kindly provided by Dr. Moshe Flaishman, Volcani ARO, Israel; Mali *et al.*, 2013) was placed under the control of the *A. thaliana* ubiquitin promoter, along with the NPTII gene under the CaMV 35S promoter and cloned into pCGN. This construct, pCGN-UbqP:*hCas9*/35S:NPTII, was introduced into *Agrobacterium tumefaciens* strain AGL0 (Lazo *et al.*, 1991). The target gene sequences (*LCY-ε*, *uGGP1*, *uGGP2*, *CCD4a*) were verified by Sanger sequencing in the 'Noga' cultivar and compared with the published lettuce genome (Verwaaijen *et al.*, 2018). gRNAs were designed using the CRISPOR web tool, prioritizing gene specificity to avoid off-target editing (Concordet and Haeussler, 2018). Each gRNA was cloned separately into the pTRV2 vector, creating pTRV2-*LCY-ε*, pTRV2-*uGGP*, pTRV2-*CCD4a*. All constructs were introduced into *Agrobacterium tumefaciens* strain AGL0 (Lazo *et al.*, 1991) and were then used to transform Cas9-expressing lettuce explants (Skaliter *et al.*, 2024), generating gene-edited lines for *LCY-ε* (L1, L2 and L3), *uGGP1/2* (A1, A2, A3 and A4) and *CCD4a* (C1, C2 and C3).

Generation of Cas9-expressing 'Noga' lettuce plants and gene-edited lines

'Noga' lettuce seeds were surface-sterilized and sown on germination medium, incubated under a 12 h light/dark photoperiod at 22 °C for 5 days. Cotyledon explants were transformed with the UbqP:*hCas9*/35S:NPTII construct via *A. tumefaciens*

(Curtis *et al.*, 1994). Plantlets with well-developed shoots and roots were sampled for DNA extraction and acclimated in greenhouse conditions. TRV vectors were used to generate genome-edited lettuce (Skaliter *et al.*, 2024). To ensure the heredity of induced mutations, gene-edited plantlets (generation M0) were grown to maturity and were allowed to self-pollinate to generate seeds; these were sown (generation M1) and allowed to self-pollinate again. Characterization procedures were performed in sequence-verified homozygous generation M2 plants.

Crossing method and lineage of multi-gene-edited plants

Cross-pollination was performed as follows: On the day of anthesis, typically just after dawn, flowers designated as females were sterilized by introducing 5–10 µL of double-distilled water into the yet-closed buds using a pipette tip. The flowers were then allowed to open and dry completely. Once dry, flowers from male pollen donors were gently rubbed against the sterilized female flowers to facilitate fertilization. The fertilized flowers were marked, and seeds were collected separately from each type of cross.

To generate the *LCY-ε*/*uGGP2* mutant population L2A4, lines L2 (*LCY-ε*) and A4 (*uGGP2*) were crossed. The resulting F1 offsprings were selfed, and this F2 population was screened via sequencing to identify plants homozygous for the *LCY-ε* knockout mutation, with varying allele combinations for *uGGP2* (wild-type, heterozygous or homozygous).

For the creation of the multi-gene-edited population (LCA), two separate crosses were performed: lines L3 (*LCY-ε*) with C3 (*CCD4a*) and lines L2 (*LCY-ε*) with A2 (*uGGP1 uGGP2*). The F1 progeny from these crosses (L3 × C3 and L2 × A2) were then crossed with each other. The F2 offspring were selfed, and the F3 population was screened by sequencing to identify plants homozygous for knockout mutations in both *LCY-ε* and *CCD4a*, heterozygous for *uGGP2* and with varying allele combinations for *uGGP1* (wild-type, heterozygous or homozygous).

Pigment extraction and HPLC analysis

Samples were taken from 2 to 3 different middle leaves of 2-month-old lettuce plants. Two hundred milligrams of tissue were weighed, frozen in liquid nitrogen and stored at −80 °C until further analysis. Carotenoids and chlorophylls were extracted with 600 µL of acetone using a bead beater and then dried under a stream of nitrogen. The dried extracts were dissolved in 300 µL of acetone. Carotenoids were separated using high-performance liquid chromatography (HPLC) on a Waters system, comprising a Waters 600 pump, a Waters 996 photodiode array detector and a Waters 717 plus autosampler (Waters, Milford, MA). The stationary phase was a Spherisorb® ODS2 C18 reversed-phase column (5 µm silica, 3.2 mm × 250 mm) from Phenomenex® (Torrance, CA). The mobile phase followed a solvent gradient detailed in Table S3, with a constant flow rate of 1.6 mL/min. Absorbance spectra from 200 to 700 nm were recorded at a rate of one full spectrum per second. Carotenoids were identified based on their characteristic retention times, verified using standards and distinctive absorption spectra. Lactucaxanthin was identified according to expected retention time and mass spectra (Gopal *et al.*, 2017; Phillip and Young, 1995).

RNA extraction and real-time quantitative PCR

Total RNA was extracted from approx. 200 mg of two-month-old leaf tissue ground with liquid nitrogen using the Tri-Reagent kit (Sigma-Aldrich) and treated with RNase-free DNase I

(ThermoFisher Scientific). First-strand cDNA was synthesized using total RNA, oligo(dT) primer and reverse transcriptase ImProm-II (Promega) according to the manufacturer's instructions. Real-time quantitative PCR (qRT-PCR) was performed for 35 cycles (95 °C for 5 min and then two steps of cycling at 95 °C for 5 s, 60 °C for 35 s) in the presence of 2X qPCR BIO SyGreen Blue Mix Hi-ROX (PCR Biosystems) on a Rotor-Gene Q cyclor (Qiagen) and CFX Opus 384 Real-Time PCR System (Bio-Rad). *ACTIN2* (*ACT2*) and *TAP42-INTERACTING PROTEIN OF 41 kDa* (*TIP41*) were used as reference genes (Sgamma et al., 2016). Quantification calculations were carried out using the $2^{-\Delta\Delta CT}$ formula as previously described (Nozue et al., 2007). The primers are shown in Table S1.

Collection of volatiles and GC–MS analysis

Volatile organic compound analysis was performed as described by Skaliter et al. (2021) with the following modifications: 5 g of fully expanded, two to four middle leaves from 2-month-old lettuce plants were ground in liquid nitrogen using a mortar and pestle. The resulting powder was transferred into a 50 mL glass beaker, which was then placed in a jar. There were three or four biological replicates for each genotype (*CCD4a* mutant experiment or *LCY-e* mutant experiment, respectively). Volatiles were collected for 18 h using columns connected to a vacuum pump with a flow rate of 2 L/min. Trapped volatiles were eluted with 900 µL hexane and 450 µL acetone. Isobutyl benzene was used as an internal standard. GC–MS analyses of eluted volatiles were performed as described by Skaliter et al. (2021).

Pulse-amplitude modulated (PAM) chlorophyll fluorescence measurements

Chlorophyll fluorescence parameters were measured using a Maxi Imaging PAM fluorometer (Heinz Walz GmbH, Germany) on ~3 cm leaf segments from the tips of middle leaves of two-month-old mutant and non-edited plants ($n = 4$) at 25 °C. Both induction and light curves were recorded. The leaf samples were dark-adapted for 20 min before measurements. Initial fluorescence (F_0) and maximum fluorescence (F_m) were recorded before and after a saturating light pulse (6000 µmol photons/m²/s for 600 ms). After a subsequent 40-s dark period, actinic light (530 µmol photons/m²/s) was applied to establish steady-state fluorescence (F_V). $F_{m'}$ was measured every 20 s using additional saturating pulses superimposed on the actinic light. Light curves were recorded with incremental actinic light from 0 to 926 µmol photons/m²/s for 40 s per step. Quantum efficiency of photosystem II (F_v/F_m) and NPQ were calculated as $F_v/F_m = (F_m - F_0)/F_m$ and $NPQ = (F_m - F_{m'})/F_{m'}$ (Maxwell and Johnson, 2000).

Ascorbic acid extraction and HPLC analysis

Sample preparation and metaphosphoric acid solution were performed according to Romero Rodriguez et al. (1992) with some modifications: One gram of fresh leaves from 2-month-old lettuce plants was crushed in liquid nitrogen. The resulting powder was mixed with 10 mL of 3% metaphosphoric acid containing 8% acetic acid and vigorously vortexed. The mixture was incubated for 15 min at room temperature with constant agitation, then filtered through a 0.22 µm filter before injection into an HPLC system (Agilent Technologies) equipped with a Bio Rad Aminex HPX-87H column (300 × 7.8 mm, cat. no. 125-0140) and a cation H cartridge (30 × 4.6 mm, cat. no. 125-0129). The mobile phase consisted of deionized HPLC-grade water (0.01 N H₂SO₄) with a flow rate of 0.6 mL/min. The column temperature was maintained at 35 °C, and detection was

performed at 254 nm using the UV range for ascorbic acid. The sample volume injected was 5–10 µL.

Sequence alignment and phylogenetic analysis

uGGP1 and uGGP2 nucleotide and amino acid sequences were aligned using the EMBOSS Needle tool (Madeira et al., 2024). In order to create the CCD4 phylogenetic tree, protein sequences were aligned using the ClustalW algorithm (Larkin et al., 2007) implemented in MEGA11 using default parameters (gap opening penalty 10.00; gap extension penalty 0.20; Tamura et al., 2021). Phylogenetic analysis was performed in MEGA11 using the maximum likelihood method with default settings (1000 bootstraps; Jones-Taylor-Thornton matrix-based model). All gene accession numbers used in this study are found in Table S5.

Carbon and nitrogen analysis

Samples (1 g) were collected from two to three middle leaves of 2-month-old multi-gene-edited plants (LCA population). The leaves were oven-dried at 60 °C for 72 h until fully desiccated, then milled into a fine powder. Five milligrams of the homogenized powdered sample were analysed using a Flash2000 CN Elemental Analyzer (Thermo Scientific, Milan, Italy; Dovrat et al., 2020).

Statistics

Statistical analyses were performed using JMP Pro 17 (SAS Institute).

Author Contributions

YL planned and designed the research, performed the experiments, analysed the data and wrote the manuscript. ELL and DA performed the experiments. TMB, VT, TM, ES and YY performed the experiments and analysed the data. AS, DC and JH wrote the manuscript. AV planned and designed the research and wrote the manuscript. All authors revised the manuscript and approved the final version.

Acknowledgements

We thank Amos Nir from Hazera Ltd. for providing plant material and for useful advice. We thank Elena Shklarman, Arik Honig and Ira Marton for their helpful guidance with experimental procedures. YL was supported by Israel's Ministry of Science and Technology's 'Golda Meir' Scholarship for Women in Science in the Academy and Industry (no. 7500158). This work was supported by the Chief Scientist of the Israel Ministry of Agriculture and Rural Development (grant no. 12-01-0037). AV is an incumbent of the Wolfson Chair in Floriculture and work in the laboratory is supported by The National Center for Genome Editing in Agriculture (no. 20-01-0209).

Data availability statement

The data that supports the findings of this study are available in the supplementary material of this article.

References

- Ahmed, H.A., Yu-Xin, T. and Qi-Chang, Y. (2020) Optimal control of environmental conditions affecting lettuce plant growth in a controlled environment with artificial lighting: a review. *South African J. Bot.* **130**, 75–89.

- Ahrazem, O., Trapero, A., Gómez, M.D., Rubio-Moraga, A. and Gómez-Gómez, L. (2010) Genomic analysis and gene structure of the plant carotenoid dioxygenase 4 family: a deeper study in *Crocus sativus* and its allies. *Genomics* **96**, 239–250.
- Amna, Qamar, S., Tantray, A.Y., Bashir, S.S., Zaid, A. and Wani, S.H. (2020) Golden rice: genetic engineering, promises, present status and future prospects. In *Rice Research for Quality Improvement: Genomics and Genetic Engineering*, Vol. **2**, pp. 581–604. Singapore: Springer Singapore.
- Bai, S., Tuan, P.A., Tatsuki, M., Yaegaki, H., Ohmiya, A., Yamamizo, C. and Moriguchi, T. (2016) Knockdown of Carotenoid Cleavage Dioxygenase 4 (CCD4) via virus-induced gene silencing confers yellow coloration in peach fruit: evaluation of gene function related to fruit traits. *Plant Mol. Biol. Report.* **34**, 257–264.
- Brychkova, G., de Oliveira, C.L., Gomes, L.A.A., de Souza Gomes, M., Fort, A., Esteves-Ferreira, A.A., Sulpice, R. et al. (2023) Regulation of carotenoid biosynthesis and degradation in lettuce (*Lactuca sativa* L.) from seedlings to harvest. *Int. J. Mol. Sci.* **24**, 10310.
- Camarena, V. and Wang, G. (2016) The epigenetic role of vitamin C in health and disease. *Cell. Mol. Life Sci.* **73**, 1645–1658.
- Carazo, A., Macáková, K., Matoušová, K., Krčmová, L.K., Protti, M. and Mladěnka, P. (2021) Vitamin a update: forms, sources, kinetics, detection, function, deficiency, therapeutic use and toxicity. *Nutrients* **13**, 703.
- Concordet, J.P. and Haeussler, M. (2018) CRISPOR: intuitive guide selection for CRISPR/Cas9 genome editing experiments and screens. *Nucleic Acids Res.* **46**, W242–W245.
- Cunningham, J. and Gantt, E. (2001) One ring or two? Determination of ring number in carotenoids by lycopene ϵ -cyclases. *Proc. Natl. Acad. Sci. USA* **98**, 2905–2910.
- Curtis, I.S., Power, J.B., Blackhall, N.W., De Laat, A.M.M. and Davey, M.R. (1994) Genotype-independent transformation of lettuce using agrobacterium tumefaciens. *J. Exp. Bot.* **45**, 1441–1449.
- Dall'Osto, L., Lico, C., Alric, J., Giuliano, G., Havaux, M. and Bassi, R. (2006) Lutein is needed for efficient chlorophyll triplet quenching in the major LHCII antenna complex of higher plants and effective photoprotection in vivo under strong light. *BMC Plant Biol.* **6**, 1–20.
- DellaPenna, D. (1999) Carotenoid synthesis and function in plants: insights from mutant studies in Arabidopsis. *Pure Appl. Chem.* **71**, 2205–2212.
- Demmig-Adams, B. (1990) Carotenoids and photoprotection in plants: a role for the xanthophyll zeaxanthin. *BBA-Bioenergetics* **1020**, 1–24.
- Demmig-Adams, B., Garab, G. and Adams, W., III (2014) *Non-Photochemical Quenching and Energy Dissipation in Plants, Algae and Cyanobacteria*. Dordrecht: Springer Netherlands.
- Deslous, P., Bournonville, C., Decros, G., Okabe, Y., Mauxion, J.-P., Jorly, J., Gadin, S. et al. (2021) Overproduction of ascorbic acid impairs pollen fertility in tomato. *J. Exp. Bot.* **72**, 3091–3107.
- Diretto, G., Tavazza, R., Welsch, R., Pizzichini, D., Mourgues, F., Papacchioli, V., Beyer, P. et al. (2006) Metabolic engineering of potato tuber carotenoids through tuber-specific silencing of lycopene epsilon cyclase. *BMC Plant Biol.* **6**, 13.
- Dovrat, G., Bakhshian, H., Masci, T. and Sheffer, E. (2020) The nitrogen economic spectrum of legume stoichiometry and fixation strategy. *New Phytol.* **227**, 365–375.
- Drouin, G., Godin, J.-R. and Page, B. (2011) The genetics of vitamin C loss in vertebrates. *Curr. Genomics* **12**, 371–378.
- Falchi, R., Vendramin, E., Zanon, L., Scalabrini, S., Cipriani, G., Verde, I., Vizzotto, G. et al. (2013) Three distinct mutational mechanisms acting on a single gene underpin the origin of yellow flesh in peach. *Plant J.* **76**, 175–187.
- Ferland, G. and Sadowski, J.A. (1992) Vitamin K1 (Phylloquinone) content of green vegetables: effects of plant maturation and geographical growth location. *J. Agric. Food Chem.* **40**, 1874–1877.
- Gargaro, M., Murphy, R.J. and Harris, Z.M. (2023) Let-us investigate; a meta-analysis of influencing factors on lettuce crop yields within controlled-environment agriculture systems. *Plan. Theory* **12**, 2623.
- Gopal, S.S., Lakshmi, M.J., Sharavana, G., Sathaiah, G., Sreerama, Y.N. and Baskaran, V. (2017) Lactucaxanthin-a potential anti-diabetic carotenoid from lettuce (*Lactuca sativa*) inhibits α -amylase and α -glucosidase activity in vitro and in diabetic rats. *Food Funct.* **8**, 1124–1131.
- Grune, T., Lietz, G., Palou, A., Ross, A.C., Stahl, W., Tang, G. et al. (2010) β -Carotene As an Important Vitamin A Source for Humans. *J. Nutr.* **140**, 2268–2285.
- Huang, F.C., Molnár, P. and Schwab, W. (2009) Cloning and functional characterization of carotenoid cleavage dioxygenase 4 genes. *J. Exp. Bot.* **60**, 3011–3022.
- Huo, H., Dahal, P., Kunusoth, K., McCallum, C.M. and Bradford, K.J. (2013) Expression of 9-cis-epoxycarotenoid dioxygenase4 is essential for thermoinhibition of lettuce seed germination but not for seed development or stress tolerance. *Plant Cell* **25**, 884–900.
- Jiang, L., Strobbe, S., Van Der Straeten, D. and Zhang, C. (2021) Regulation of plant vitamin metabolism: backbone of biofortification for the alleviation of hidden hunger. *Mol. Plant* **14**, 40–60.
- Johnson, E.J. (2014) Role of lutein and zeaxanthin in visual and cognitive function throughout the lifespan. *Nutr. Rev.* **72**, 605–612.
- Kaur, N., Alok, A., Shivani, Kumar, P., Kaur, N., Awasthi, P., Chaturvedi, S. et al. (2020) CRISPR/Cas9 directed editing of lycopene epsilon-cyclase modulates metabolic flux for β -carotene biosynthesis in banana fruit. *Metab. Eng.* **59**, 76–86.
- Ke, Q., Kang, L., Kim, H.S., Xie, T., Liu, C., Ji, C.Y., Kim, S.H. et al. (2019) Down-regulation of lycopene ϵ -cyclase expression in transgenic sweetpotato plants increases the carotenoid content and tolerance to abiotic stress. *Plant Sci.* **281**, 52–60.
- Khanam, U.K.S., Oba, S., Yanase, E. and Murakami, Y. (2012) Phenolic acids, flavonoids and total antioxidant capacity of selected leafy vegetables. *J. Funct. Foods* **4**, 979–987.
- Kim, M.J., Moon, Y., Kopsell, D.A., Park, S., Tou, J.C. and Waterland, N.L. (2016a) Nutritional value of crisphead 'Iceberg' and romaine lettuces (*Lactuca sativa* L.). *J. Agric. Sci.* **8**, 1.
- Kim, M.J., Moon, Y., Tou, J.C., Mou, B. and Waterland, N.L. (2016b) Nutritional value, bioactive compounds and health benefits of lettuce (*Lactuca sativa* L.). *J. Food Compos. Anal.* **49**, 19–34.
- Kumar, D., Yadav, A., Ahmad, R., Dwivedi, U.N. and Yadav, K. (2022) CRISPR-based genome editing for nutrient enrichment in crops: a promising approach toward global food security. *Front. Genet.* **13**, 1–12.
- Laing, W.A., Martínez-Sánchez, M., Wright, M.A., Bulley, S.M., Brewster, D., Dare, A.P., Rassam, M. et al. (2015) An upstream open reading frame is essential for feedback regulation of ascorbate biosynthesis in Arabidopsis. *Plant Cell* **27**, 772–786.
- Larkin, M.A., Blackshields, G., Brown, N.P., Chenna, R., McGettigan, P.A., McWilliam, H., Valentin, F. et al. (2007) Clustal W and Clustal X version 2.0. *Bioinformatics* **23**, 2947–2948.
- Lazo, G.R., Stein, P.A. and Ludwig, R.A. (1991) A DNA transformation-competent Arabidopsis genomic library in agrobacterium. *BioTechnology* **9**, 963–967.
- Li, T., Yang, X., Yu, Y., Si, X., Zhai, X., Zhang, H., Dong, W. et al. (2018) Domestication of wild tomato is accelerated by genome editing. *Nat. Biotechnol.* **36**, 1160–1163.
- Lokstein, H., Renger, G. and Götz, J.P. (2021) Photosynthetic light-harvesting (Antenna) complexes-structures and functions. *Molecules* **26**(11), 3378. <https://doi.org/10.3390/molecules26113378>
- Lynch, S.R. and Cook, J.D. (1980) Interaction of vitamin C and iron. *Ann. N. Y. Acad. Sci.* **355**, 32–44.
- Lyzenga, W.J., Pozniak, C.J. and Kagale, S. (2021) Advanced domestication: harnessing the precision of gene editing in crop breeding. *Plant Biotechnol. J.* **19**, 660–670.
- Madeira, F., Madhusoodanan, N., Lee, J., Eusebi, A., Niewielska, A., Tivey, A.R.N., Lopez, R. et al. (2024) The EMBL-EBI job dispatcher sequence analysis tools framework in 2024. *Nucleic Acids Res.* **52**, W521–W525.
- Magome, H., Arai, M., Oyama, K., Nishiguchi, R. and Takakura, Y. (2023) Multiple loss-of-function mutations of carotenoid cleavage dioxygenase 4 reveal its major role in both carotenoid level and apocarotenoid composition in flue-cured mature tobacco leaves. *Sci. Rep.* **13**, 12992.
- Mali, P., Yang, L., Esvelt, K.M., Aach, J., Guell, M., DiCarlo, J.E., Norville, J.E. et al. (2013) RNA-guided human genome engineering via Cas9. *Science* (80-) **339**, 823–826.
- Maxwell, K. and Johnson, G.N. (2000) Chlorophyll fluorescence—a practical guide. *J. Exp. Bot.* **51**, 659–668.

- Medina-Lozano, I. and Díaz, A. (2022) Applications of genomic tools in plant breeding: crop biofortification. *Int. J. Mol. Sci.* **23**, 23.
- Mellidou, I. and Kanellis, A.K. (2017) Genetic control of ascorbic acid biosynthesis and recycling in horticultural crops. *Front. Chem.* **5**, 50.
- Meng, K., Eldar-Liebreich, M., Nawade, B., Yahyaa, M., Shaltiel-Harpaz, L., Coll, M., Sadeh, A. et al. (2023) Analysis of apocarotenoid volatiles from lettuce (*Lactuca sativa*) induced by insect herbivores and characterization of carotenoid cleavage dioxygenase gene. *3 Biotech* **13**, 1–11.
- Mishra, A. and Pandey, V.P. (2024) CRISPR/Cas system: a revolutionary tool for crop improvement. *Biotechnol. J.* **19**, 1–23.
- Morand-Laffargue, L., Hirschberg, J., Halimi, C., Desmarchelier, C. and Borel, P. (2023) The zeaxanthin present in a tomato line rich in this carotenoid is as bioavailable as that present in the food sources richest in this Xanthophyll. *Food Res. Int.* **168**, 112751.
- Morelli, L., Perez-Colao, P., Reig-Lopez, D., Di, X., Llorente, B. and Rodriguez-Concepcion, M. (2024) Boosting pro-vitamin A content and bioaccessibility in leaves by combining engineered biosynthesis and storage pathways with high-light treatments. *Plant J.* **119**, 2951–2966.
- Mou, B. (2005) Genetic variation of beta-carotene and lutein contents in lettuce. *J. Am. Soc. Hortic. Sci.* **130**, 870–876.
- Naqvi, S., Zhu, C., Farre, G., Ramessar, K., Bassie, L., Breitenbach, J., Conesa, D.P. et al. (2009) Transgenic multivitamin corn through biofortification of endosperm with three vitamins representing three distinct metabolic pathways. *Proc. Natl. Acad. Sci. USA* **106**, 7762–7767.
- Nozue, K., Covington, M.F., Duek, P.D., Lorrain, S., Fankhauser, C., Harmer, S.L. and Maloof, J.N. (2007) Rhythmic growth explained by coincidence between internal and external cues. *Nature* **448**, 358–361.
- Ntagkas, N., Woltering, E.J. and Marcelis, L.F.M. (2018) Light regulates ascorbate in plants: an integrated view on physiology and biochemistry. *Environ. Exp. Bot.* **147**, 271–280.
- Ohmiya, A., Kishimoto, S., Aida, R., Yoshioka, S. and Sumitomo, K. (2006) Carotenoid Cleavage Dioxygenase (CmCCD4a) contributes to white color formation in chrysanthemum petals. *Plant Physiol.* **142**, 1193–1201.
- Paciolla, C., Fortunato, S., Dipierro, N., Paradiso, A., De Leonardis, S., Mastropasqua, L. and de Pinto, M.C. (2019) Vitamin C in plants: from functions to biofortification. *Antioxidants* **8**, 519.
- Park, S., Shi, A. and Mou, B. (2020) Genome-wide identification and expression analysis of the CBF/DREB1 gene family in lettuce. *Sci. Rep.* **10**, 1–14.
- Phillip, D. and Young, A.J. (1995) Occurrence of the carotenoid lactucaxanthin in higher plant LHC II. *Photosynth. Res.* **43**, 273–282.
- Pogson, B.J., Niyogi, K.K., Björkman, O. and DellaPenna, D. (1998) Altered xanthophyll compositions adversely affect chlorophyll accumulation and nonphotochemical quenching in Arabidopsis mutants. *Proc. Natl. Acad. Sci. USA* **95**, 13324–13329.
- Richaud, D., Stange, C., Gadaleta, A., Colasuonno, P., Parada, R. and Schwember, A.R. (2018) Identification of Lycopene Epsilon Cyclase (LCYE) gene mutants to potentially increase β -carotene content in durum wheat (*Triticum turgidum* L. ssp. durum) through TILLING. *PLoS One* **13**, 1–17.
- Romero Rodriguez, M.A., Vazquez Oderiz, M.L., Lopez Hernandez, J. and Simal Lozano, J. (1992) Determination of vitamin C and organic acids in various fruits by Hplc. *J. Chromatogr. Sci.* **30**, 433–437.
- Rosas-Saavedra, C. and Stange, C. (2016) Biosynthesis of carotenoids in plants: enzymes and color. In *Carotenoids in Nature: Biosynthesis, Regulation and Function* (Stange, C., ed), pp. 35–69. Cham: Springer International Publishing.
- Rottet, S., Besagni, C. and Kessler, F. (2015) The role of plastoglobules in thylakoid lipid remodeling during plant development. *Biochim. Biophys. Acta Bioenerg.* **1847**, 889–899.
- Rowe, S. and Carr, A.C. (2020a) Factors affecting vitamin C status and prevalence of deficiency: a global health perspective. *Nutrients* **1**, 1–19.
- Rowe, S. and Carr, A.C. (2020b) Global vitamin C status and prevalence of deficiency: a cause for concern? *Nutrients* **12**, 1–20.
- Sajilata, M.G., Singhal, R.S. and Kamat, M.Y. (2008) The carotenoid pigment zeaxanthin – a review. *Proc. Comp. Rev. Food Sci. Food Safety* **7**, 29–49.
- Sajovic, J., Meglič, A., Glavač, D., Markelj, Š., Hawlina, M. and Fakin, A. (2022) The role of vitamin A in retinal diseases. *Int. J. Mol. Sci.* **23**, 1–27.
- Sawada, Y., Aoki, M., Nakaminami, K., Mitsuhashi, W., Tatematsu, K., Kushi, T., Koshihara, T. et al. (2008) Phytochrome- and gibberellin-mediated regulation of abscisic acid metabolism during germination of photoblastic lettuce seeds. *Plant Physiol.* **146**, 1386–1396.
- Scharff, L.B., Saltenis, V.L.R., Jensen, P.E., Baekelandt, A., Burgess, A.J., Burow, M., Ceriotti, A. et al. (2022) Prospects to improve the nutritional quality of crops. *Food Energy Secur.* **11**, 1–14.
- Sgamma, T., Pape, J., Massiah, A. and Jackson, S. (2016) Selection of reference genes for diurnal and developmental time-course real-time PCR expression analyses in lettuce. *Plant Methods* **12**, 1–9.
- Siefermann-Harms, D., Hertzberg, S., Borch, G. and Liaaen-Jensen, S. (1981) Lactucaxanthin, an ϵ,ϵ -Carotene-3,3'-diol from *Lactuca sativa*. *Phytochemistry* **20**, 85–88.
- Simkin, A.J. (2021) Carotenoids and apocarotenoids in plants: their role in plant development, contribution to the flavour and aroma of fruits and flowers, and their nutraceutical benefits. *Plan. Theory* **10**, 2321.
- Skaliter, O., Kitsberg, Y., Sharon, E., Shklarman, E., Shor, E., Masci, T., Yue, Y. et al. (2021) Spatial patterning of scent in petunia corolla is discriminated by bees and involves the ABCG1 transporter. *Plant J.* **106**, 1746–1758.
- Skaliter, O., Bednarczyk, D., Shor, E., Shklarman, E., Manasherova, E., Aravena-Calvo, J., Kerzner, S. et al. (2024) The R2R3-MYB transcription factor EVER controls the emission of petunia floral volatiles by regulating epicuticular wax biosynthesis in the petal epidermis. *Plant Cell* **36**, 174–193.
- Smirnoff, N. and Wheeler, G.L. (2000) Ascorbic acid in plants: biosynthesis and function. *Crit. Rev. Biochem. Mol. Biol.* **35**, 291–314.
- Tamura, K., Stecher, G. and Kumar, S. (2021) MEGA11: molecular evolutionary genetics analysis version 11. *Mol. Biol. Evol.* **38**, 3022–3027.
- Varghese, R., Kumar, S.U., Doss, C.G.P. and Ramamoorthy, S. (2021) Unraveling the versatility of CCD4: metabolic engineering, transcriptomic and computational approaches. *Plant Sci.* **310**, 110991.
- Verwaaijen, B., Wibberg, D., Nelkner, J., Gordin, M., Rupp, O., Winkler, A., Bremges, A. et al. (2018) Assembly of the *Lactuca sativa*, L. Cv. Tizian draft genome sequence reveals differences within major resistance complex 1 as compared to the Cv. Salinas reference genome. *J. Biotechnol.* **267**, 12–18.
- Watanabe, K., Oda-Yamamizo, C., Sage-Ono, K., Ohmiya, A. and Ono, M. (2018) Alteration of flower colour in ipomoea nil through CRISPR/Cas9-mediated mutagenesis of carotenoid cleavage dioxygenase 4. *Transgenic Res.* **27**, 25–38.
- Ye, X., Al-Babili, S., Klöti, A., Zhang, J., Lucca, P., Beyer, P. and Potrykus, I. (2000) Engineering the provitamin A (β -Carotene) biosynthetic pathway into (carotenoid-free) rice endosperm. *Science (80-)* **287**, 303–305.
- Yu, B., Lydiate, D.J., Young, L.W., Schäfer, U.A. and Hannoufa, A. (2008) Enhancing the carotenoid content of *Brassica napus* seeds by downregulating lycopene epsilon cyclase. *Transgenic Res.* **17**, 573–585.
- Yu, S., Li, M., Dubcovsky, J. and Tian, L. (2022) Mutant combinations of lycopene ϵ -cyclase and β -carotene hydroxylase 2 homoeologs increased β -carotene accumulation in endosperm of tetraploid wheat (*Triticum turgidum* L.) grains. *Plant Biotechnol. J.* **20**, 564–576.
- Zhang, H., Si, X., Ji, X., Fan, R., Liu, J., Chen, K., Wang, D. et al. (2018) Genome editing of upstream open reading frames enables translational control in plants. *Nat. Biotechnol.* **36**, 894–900.
- Zheng, X., Kuijter, H.N.J. and Al-Babili, S. (2021) Carotenoid biofortification of crops in the CRISPR Era. *Trends Biotechnol.* **39**, 857–860.

Supporting information

Additional supporting information may be found online in the Supporting Information section at the end of the article.

Figure S1 GC–MS analysis of β -ionone levels in mutant line L3 and non-edited control plants.

Figure S2 Relative expression of carotenoid biosynthetic pathway genes in *LCY- ϵ* knockout mutants and non-edited control plants.

Figure S3 Protein alignment of the upstream ORF of lettuce GGP1 (uGGP1) and GGP2 (uGGP2).

Figure S4 Nucleotide and amino acid alignment of lettuce uGGP1 and uGGP2.

Figure S5 Representative HPLC profiles of carotenoid extracts from the leaves of non-edited (control) and multi-gene-edited lettuce plants.

Figure S6 Carbon and nitrogen content in two-month-old leaves of multi-gene-edited lettuce plants.

Table S1 Leaf number and length of *LCY-e* knockout mutants and non-edited control plants.

Table S2 Whole plant mass, leaf number and leaf length in *CCD4a* gene-edited lettuce lines C1, C2 and C3 compared to non-edited (NE) control plants.

Table S3 Conditions of solvent gradient used for carotenoid separation by HPLC.

Table S4 Primers used in this study.

Table S5 Gene accession numbers.